

---

## Femtosecond Excited-State Dynamics of a Conjugated Ladder Polymer

Among the known classes of nonlinear optical materials,  $\pi$ -conjugated polymers are very attractive because of their large, third-order optical susceptibilities and ultrafast response times.<sup>1–5</sup> The large optical nonlinearity of conjugated polymers has long been recognized as arising from the  $\pi$ -electron delocalization along the polymer chains.<sup>2</sup> Recently, aromatic heterocyclic ladder-type polymers, such as poly(benzimidazobenzophenanthroline) ladder (BBL) and semi-ladder (BBB), have received growing attention as a new class of nonlinear optical (NLO) polymers<sup>3–5</sup> because of their desirable physical properties and their ready processibility into good optical-quality thin films.<sup>6</sup> For example, BBL has an excellent thermal stability up to 700°C in a nitrogen atmosphere (~650°C in air) and has good mechanical properties in the form of films or fibers;<sup>6</sup> both of these features suggest that the optical damage threshold may be very high. The rigid, planar, “double stranded,” and quasi-two-dimensional structure of BBL (inset of Fig. 60.22) suggests maximum  $\pi$ -electron delocalization, leading to a large, third-order optical susceptibility  $\chi^{(3)}$  as found in picosecond degenerate four-wave mixing (DFWM)<sup>4</sup> and picosecond third-harmonic-generation (THG) experiments.<sup>5</sup> However, the temporal resolution of the nonlinear optical response of BBL was limited to 30 ps by the experimental equipment in both of these prior studies.<sup>4,5</sup>

The excited-state dynamics of conjugated polymers has been extensively studied following the theoretical prediction that new intragap states can be generated by photoexcitation within an optical phonon cycle (<100 fs).<sup>7</sup> Because of the normally strong electron-phonon coupling in conjugated polymers, self-localized excited states are formed upon photoexcitation. Examples of these structurally relaxed states include solitons, polarons, bipolarons, and excitons.<sup>8–10</sup> These photoexcitations play a critical role in the nonlinear optical behavior of the conjugated polymers, which are often considered to be quasi-one-dimensional systems. Ultrafast transient spectroscopy studies of photoexcitations in conjugated polymers have been widely reported on single-stranded, non-ladder-type polymers such as trans-polyacetylene (PA), polydiacetylenes (PDA's), polythiophenes (PT's), poly(p-phenylene vinylenes) (PPV's), and poly(thiophene vinylenes) (PTV's).<sup>11–19</sup> The unique topological features of BBL among the known conjugated polymers give rise to novel charge transport properties.<sup>20</sup> This and the recent interest in its nonlinear optical and optoelectronic properties make this ladder polymer an excellent candidate for a detailed investigation of its ultrafast excited-state dynamics.

In this article we report studies of the time-resolved femtosecond (fs) dynamics following photoexcitation in a BBL thin film. The experimental results reveal a sub-picosecond response of the optical nonlinearity. We show that the nonlinear excitations in the ladder polymer are similar to those observed in single-stranded conjugated polymers.

The measurements were performed at room temperature on a BBL thin-film sample. The sample was spin coated on a sapphire substrate and was approximately 500 Å thick. The details of the synthesis of BBL and fabrication of thin films have been described elsewhere.<sup>6</sup> An amplified colliding-pulse mode-locked (CPM) laser system was employed for the pump and probe measurements. Light pulses of approximately 100 fs centered at 620 nm were generated from the CPM laser and further amplified by a copper vapor laser-pumped dye amplifier to the energy level of about 1  $\mu$ J per pulse at a repetition rate of 8.7 kHz. Ninety percent of the amplified pulses were focused onto an ethylene glycol jet to generate a white-light continuum that provided probe pulses tunable from 500 nm to 900 nm. The remaining 10% were used as pump pulses. The intensity of the pump pulses on the sample was ~1 GW/cm<sup>2</sup>. A cross-polarization arrangement of the pump and probe beams was used to eliminate the coherent artifact. The BBL sample exhibited excellent stability throughout the experiments, and no signal degradation was found.

Figure 60.22 shows the room-temperature linear absorption spectrum and the chemical structure of BBL. The onset of major optical absorption occurs at 690 nm (1.8 eV). The pump pulses (2 eV) used in the experiments were well above the optical gap. The results of the pump- and continuum-probe

experiment on BBL are shown in Fig. 60.23. The transient photoinduced probe transmission change ( $\Delta T/T$ ) was measured as a function of the probe time delay. For probe wavelengths above the optical gap ( $\lambda = 620$  nm and  $650$  nm), increased transmission (bleaching) was observed. For probe below the gap ( $\lambda > 690$  nm), photoinduced absorption was observed. Both bleaching and absorption signals appear promptly (within our time resolution) following the excitation. Figure 60.24 shows the fit of the bleaching and absorption signals for three different probe wavelengths. Neither bleaching nor absorption decay can be fitted by a single exponential function. The decay of the bleaching signal is best fitted to a biexponential function and a constant term of the form  $\Delta T/T = A \exp(-t/\tau_1) + B \exp(-t/\tau_2) + C$ . For the 620-nm probe, the initial fast decay has a time constant  $\tau_1 = 0.39$  ps, whereas the slow component is  $\tau_2 = 2.11$  ps. The best fit to all the transient absorption traces is a biexponential function with a fast component and a slow component of the form  $\Delta T/T = A \exp(-t/\tau_1) + B \exp(-t/\tau_2)$ . The decay of the photo-induced absorption is much slower than that of the photo-induced bleaching and is also wavelength dependent. The slowest decay occurs at 770 nm when  $\tau_1 = 1.03$  ps and  $\tau_2 = 29.5$  ps. The results of fitting the photoinduced bleaching and absorption data are summarized in Table 60.II.

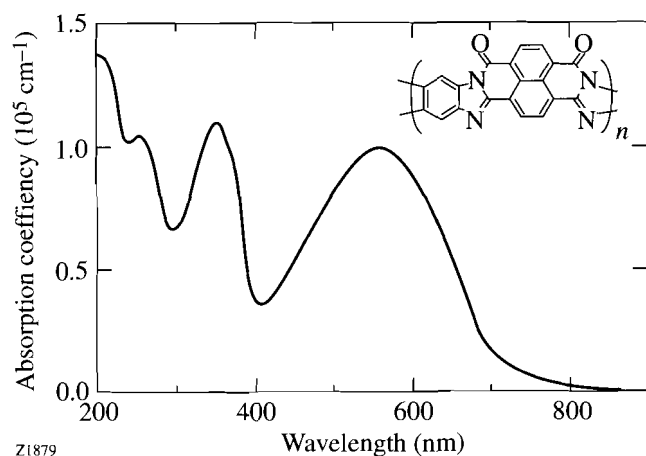


Figure 60.22  
The room-temperature absorption spectrum and the chemical structure (inset) of BBL.

The ultrafast dynamics can be explained by the photogeneration and decay of self-trapped excitons (STE's) or polaron-excitons.<sup>16,17</sup> In nondegenerated ground-state polymers, photogenerated electron-hole pairs are confined through the preferred sense of bond alternation on the polymer chain and cannot be totally separated. The main product of intra-

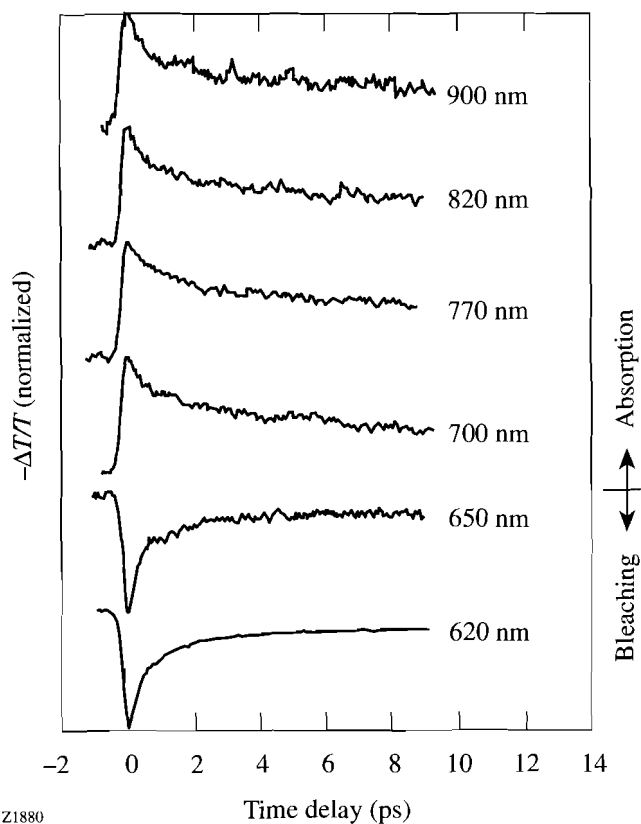


Figure 60.23  
Transient photoinduced transmission change ( $\Delta T/T$ ) measured as a function of the probe delay time at different probe wavelengths following excitation at 620 nm. The traces have been displaced vertically for clarity. Bleaching is observed above  $E_g$  and induced absorption below  $E_g$ .

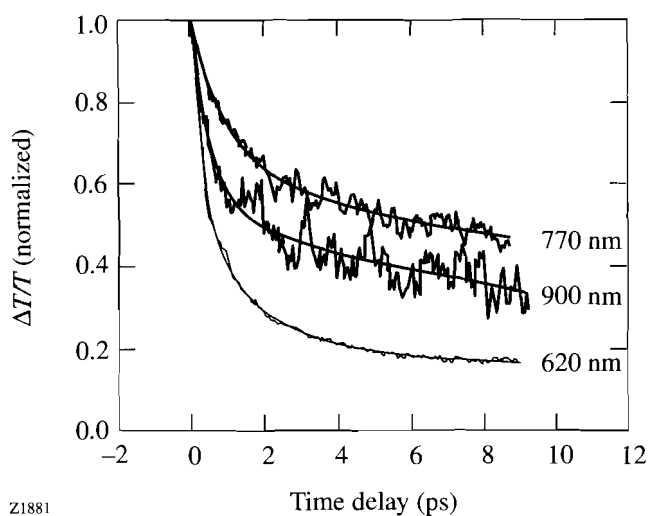
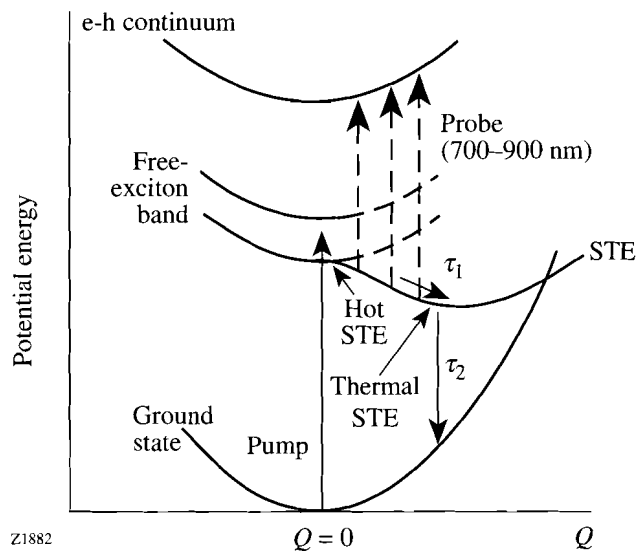


Figure 60.24  
Fitting of the decay curves of the bleaching signal (probe at 620 nm) and absorption signals (probe at 770 nm and 900 nm). The smooth curves are fits as described in the text.

Table 60.II The lifetimes resulting from fitting of the decay curves at different probing wavelengths  $\lambda$ .

$\lambda$ (nm)	$\tau_1$ (ps)	$\tau_2$ (ps)
620	$0.39 \pm 0.01$	$2.11 \pm 0.1$
650	$0.25 \pm 0.02$	$1.46 \pm 0.1$
700	$0.60 \pm 0.05$	$15.3 \pm 0.5$
770	$1.03 \pm 0.06$	$29.5 \pm 2.2$
820	$0.59 \pm 0.05$	$18.9 \pm 1.0$
900	$0.59 \pm 0.05$	$20.5 \pm 1.6$



Z1882

Figure 60.25

The adiabatic potential energy curves of the excited and ground states plotted against the lattice deformation  $Q$ .

chain photoexcitation is neutral, self-trapped excitons.<sup>10</sup> Kobayashi *et al.* studied photoexcitations in polydiacetylene and explained their results by the self-trapped exciton model.<sup>16,17</sup> Greene *et al.* have studied the excitonic absorption saturation effect in polydiacetylene and explained their results by exciton phase-space filling.<sup>21</sup> Recently, Samuel *et al.* have studied the picosecond photoinduced absorption in PTV and PPV and have assigned the observed signals to polaron-excitons.<sup>22</sup> Since BBL has a nondegenerated ground state and the observed photoinduced absorption and bleaching signals in BBL resemble those in PDA and PPV, we attribute them to STE's. Other excitations such as bipolarons or triplet excitons have very little contribution to the signals within the time window (10 ps) of our experiments.

Figure 60.25 shows the adiabatic potential energy curves of the ground and excited states of the system as functions of the lattice deformation  $Q$ . The ground and excited states are represented by parabolic curves. The equilibrium lattice deformation  $Q=0$  corresponds to a perfect dimerized lattice resulting from the Peierls instability. Free excitons are created by  $\pi-\pi^*$  photoexcitation. Due to the strong electron-phonon coupling, free excitons are unstable and undergo self-trapping quickly after creation. Since in a quasi-one-dimensional system there is no barrier between the potential curves of the free excitons and the STE's, self-trapping takes place within the coupled phonon period ( $<100$  fs) and produces hot STE's.<sup>23,24</sup> The hot STE's then thermalize toward the bottom of the STE potential surface by emission of phonons. Simultaneously, the hot STE's can relax directly to the ground state. This occurs via an oscillation passing over the point where the STE potential crosses the ground state potential.<sup>16,17</sup> The initial decay of the bleaching is due to the combination of these two processes. The thermalized excitons then decay to the ground state either

radiatively or nonradiatively. We find that the characteristic decay time of STE's is of the order of 10 ps, which is much shorter than the expected radiative lifetime of STE's ( $\sim 1$  ns), indicating that the nonradiative pathways play a significant role. This is consistent with our observation of the low photoluminescence quantum yield in BBL. The nonradiative decay of STE's is considered to be either tunneling between the potential energy curves from the exciton state to the ground state or the evolution of excitons to form new intermediate species between the exciton and the ground state, such as excimers.<sup>25</sup> There is a constant component in bleaching signals that accounts for about 20% of the maximum signal. This constant component may be associated with the formation of new species, which results in a very slow recovery of the ground-state populations.

The induced absorption is assigned to the transitions from the self-trapped excitons to higher excited continuum states. Although both the bleaching signal and the absorption signal contain a fast decay component and a slow decay component, the decay of the absorption is much slower than that of the bleaching. The decay of the photoinduced absorption is also wavelength dependent, with the slowest decay at 770 nm. One possible reason for this can be seen by examining the thermalization and cooling of the hot STE's. The hot excitons reach the bottom of the potential curve in two steps. They thermalize first to form quasi-thermalized STE's by phonon emission. These quasi-thermalized excitons have still not reached the bottom of the potential curve; they cool to the bottom by

coupling with phonon modes of lower frequencies.<sup>16</sup> Thus by probing at different wavelengths, we follow the evolution of the STE's as shown in Fig. 60.25. The bleaching signal that monitors the disappearance of free excitons is due to both hot STE's and quasi-thermalized STE's. The absorption signal, however, comes mainly from thermalized or cold STE's, depending on the probing wavelength. Since the thermalized excitons are closer to the bottom of the potential curve than the hot excitons, their decay to the ground state is by tunneling through a higher and thicker potential barrier and is expected to be slower than that of hot excitons. When probing at longer wavelengths (820 nm, 900 nm), the signal comes from excitons that are hotter than those seen by probing at 770 nm; therefore, the decay should be faster, in agreement with the experimental data.

In conclusion, the dynamics of the photoexcitations in the conjugated ladder polymer BBL has been studied for the first time by femtosecond time-resolved absorption measurements. Photoinduced bleaching of the  $\pi$ - $\pi^*$  absorption band and intragap photoinduced absorption were observed. The observed excited-state decay dynamics is consistent with the self-trapped exciton model and is tentatively explained by the generation and decay of the STE's. The observed signals arise within our time resolution and feature both a fast and a slow component. The fast component is attributed to the self-trapping and thermalization of free excitons, while the slow component was assigned to the relaxation of the quasi-thermalized and/or cold STE's to other excited state species or the ground state. The difference between the decay dynamics of bleaching and absorption has been explained by the thermalization and cooling of hot STE's.

#### ACKNOWLEDGMENT

This work was supported in part by the National Science Foundation (CTS 9311741) and the Center for Photoinduced Charge Transfer. Y. Kostoulas acknowledges support of the Link Foundation.

#### REFERENCES

1. *Materials for Nonlinear Optics: Chemical Perspectives*, edited by S. R. Marder, J. E. Sohn, and G. D. Stucky (American Chemical Society, Washington, DC, 1991).
2. G. P. Agrawal, C. Cojan, and C. Flytzanis, *Phys. Rev. B* **17**, 776 (1978).
3. A. K. Agrawal *et al.*, *J. Phys. Chem.* **96**, 2837 (1992).
4. J. R. Lindle *et al.*, *Appl. Phys. Lett.* **56**, 712 (1990).
5. S. A. Jenekhe *et al.*, *Mater. Res. Soc. Symp. Proc.* **214**, 55 (1991).
6. S. A. Jenekhe and P. O. Johnson, *Macromolecules* **23**, 4419 (1990).
7. W. P. Su and J. R. Schrieffer, *Proc. Natl. Acad. Sci. USA.* **77**, 5626 (1980).
8. K. Fesser, A. R. Bishop, and D. K. Campbell, *Phys. Rev. B* **27**, 4804 (1983).
9. A. J. Heeger *et al.*, *Rev. Mod. Phys.* **60**, 781 (1988).
10. R. H. Friend, D. D. C. Bradley, and P. D. Townsend, *J. Phys. D: Appl. Phys.* **20**, 1367 (1987).
11. C. V. Shank *et al.*, *Phys. Rev. Lett.* **49**, 1660 (1982).
12. J. Orenstein, in *Handbook of Conducting Polymers*, edited by T. A. Skothein (Marcel Dekker, New York, 1986), Vol. 2, p. 1297.
13. G. M. Carter *et al.*, *Appl. Phys. Lett.* **49**, 998 (1986).
14. B. I. Green *et al.*, *Chem. Phys. Lett.* **139**, 381 (1987).
15. G. J. Blanchard *et al.*, *Chem. Phys. Lett.* **158**, 329 (1989).
16. T. Kobayashi *et al.*, *J. Opt. Soc. Am. B* **7**, 1558 (1990).
17. M. Yoshizawa, A. Yasuda, and T. Kobayashi, *Appl. Phys. B* **53**, 296 (1991).
18. J. M. Huxley *et al.*, *Appl. Phys. Lett.* **56**, 1600 (1990).
19. B. C. Hess *et al.*, *Phys. Rev. Lett.* **66**, 2364 (1991).
20. H. Mizes and E. Conwell, *Phys. Rev. B* **44**, 3963 (1991).
21. B. I. Greene *et al.*, *Phys. Rev. Lett.* **61**, 325 (1988).
22. I. D. Samuel *et al.*, *Synth. Met.* **55-57**, 15-21 (1993).
23. E. I. Rashba and M. D. Sturge, in *Excitons*, edited by E. I. Rashba and M. D. Sturge (North-Holland, Amsterdam, 1982), p. 578.
24. K. Nasu, *J. Lumin.* **38**, 90 (1987).
25. S. A. Jenekhe and J. A. Osaheni, *Science* **265**, 765 (1994).